
Limited-Memory Matrix Adaptation for Large Scale Black-box Optimization

Ilya Loshchilov

Research Group on Machine Learning
for Automated Algorithm Design
University of Freiburg, Germany
ilya.loshchilov@gmail.com

Tobias Glasmachers

Institut für Neuroinformatik
Ruhr-Universität Bochum, Germany
tobias.glasachers@ini.rub.de

Hans-Georg Beyer

Research Center Process and Product Engineering
Vorarlberg University of Applied Sciences, Dornbirn, Austria
hans-georg.beyer@fhv.at

Abstract

The Covariance Matrix Adaptation Evolution Strategy (CMA-ES) is a popular method to deal with nonconvex and/or stochastic optimization problems when the gradient information is not available. Being based on the CMA-ES, the recently proposed Matrix Adaptation Evolution Strategy (MA-ES) provides a rather surprising result that the covariance matrix and all associated operations (e.g., potentially unstable eigendecomposition) can be replaced in the CMA-ES by a updated transformation matrix without any loss of performance. In order to further simplify MA-ES and reduce its $\mathcal{O}(n^2)$ time and storage complexity to $\mathcal{O}(n \log(n))$, we present the Limited-Memory Matrix Adaptation Evolution Strategy (LM-MA-ES) for efficient zeroth order large-scale optimization. The algorithm demonstrates state-of-the-art performance on a set of established large-scale benchmarks. We explore the algorithm on the problem of generating adversarial inputs for a (non-smooth) random forest classifier, demonstrating a surprising vulnerability of the classifier.

1 Introduction

Evolution Strategies (ESs) are optimization methods originally inspired by mutation of organic beings and designed to establish “a reward-based system, to increase the probability of those changes, which lead to improvements of quality of the system” [31]. Going far beyond their biologically inspired roots, they have been developed into state-of-the-art zeroth order search methods [12]. Evolution Strategies [32] consider an objective function $f : \mathbb{R}^n \mapsto \mathbb{R}, \mathbf{x} \mapsto f(\mathbf{x})$ to be minimized by sampling $i \in \{1, \dots, \lambda\}$ candidate solutions at iteration t as

$$\mathbf{x}_i^{(t)} \leftarrow \mathbf{y}^{(t)} + \sigma^{(t)} \cdot \mathcal{N}(\mathbf{0}, \mathbf{C}^{(t)}), \quad (1)$$

where $\mathbf{y}^{(t)}$ is the current estimate of the optimum, $\mathbf{C}^{(t)} \in \mathbb{R}^{n \times n}$ is a covariance matrix initialized to the identity matrix \mathbf{I} , and $\sigma^{(t)}$ is a scaling factor for the mutation step, often referred to as the global step size. Both $\mathbf{y}^{(t)}$ and $\sigma^{(t)}$ are to be adapted or *learned* over time in Evolution Strategies. Modern ESs such as the Covariance Matrix Adaptation Evolution Strategy (CMA-ES) also include the adaptation of $\mathbf{C}^{(t)}$ [15, 14] to the shape of the local landscape, resembling second order methods. Recent theoretical studies of ES and CMA-ES from the perspective of information geometry [39, 4, 29, 5], connecting the method to natural gradient learning, have made significant progress in

understanding the principles underpinning the state-of-the-art performance of the algorithm [13]. The variety of algorithms [12] derived from and inspired by the theoretical studies helped to notice that the core component of CMA-ES, the covariance matrix itself (and covariance matrix square root operations) can be removed from the algorithm without any loss of performance [8].¹ The final algorithm called Matrix Adaptation Evolution Strategy (MA-ES [8]) is conceptually simpler and involves only matrix-matrix and matrix-vector operations, which, however, lead to $\mathcal{O}(n^3/\log(n))$ time complexity per sample (here, we show its $\mathcal{O}(n^2)$ implementation), and $\mathcal{O}(n^2)$ space complexity.

In machine learning, ESs are mainly used for direct policy search in reinforcement learning [11, 18, 36, 34], hyperparameter tuning in supervised learning, e.g., for Support Vector Machines [10, 19] and Deep Neural Networks [27]. With the steadily increasing dimensionality of real-world optimization problems, the new challenges of large-scale black-box optimization become more pronounced for CMA-ES and MA-ES due to their $\mathcal{O}(n^2)$ complexity. To address them, a number of large-scale CMA-ES variants has been proposed [23, 33, 37, 1, 26, 3] including the Limited-Memory CMA-ES (LM-CMA-ES [26]) that matches the performance of quasi-Newton methods such as L-BFGS [35] when dealing with large-scale black-box problems at a moderate cost of $\mathcal{O}(n \log(n))$ time and space complexity.

In this work, we combine the best of two worlds: inspired by LM-CMA-ES we present the Limited-Memory Matrix Adaptation Evolution Strategy (LM-MA-ES), which matches state-of-the-art results while reducing the time and space complexity of MA-ES to $\mathcal{O}(n \log(n))$ per sample.

2 Variable Metric Evolution Strategies: CMA-ES and MA-ES

Our discussion on variable metric ESs is based on Algorithm 1, which highlights the similarities and differences between CMA-ES, MA-ES, and the proposed LM-MA-ES.

The sampling of the λ candidate solutions in CMA-ES is described by eq. (1) and involves a matrix-vector product between a matrix $\sqrt{\mathbf{C}}$ and a vector \mathbf{z}_i sampled from the n -dimensional standard normal distribution. This operation (see line 7 in Algorithm 1) requires $\sqrt{\mathbf{C}}$ to be stored (hence, the quadratic in n space cost) and the matrix-vector multiplication to be performed (hence, the quadratic in n time cost). The resulting vector \mathbf{d}_i represents a direction of the so-called mutation operation. The i -th candidate solution is obtained by changing (mutating) the current estimate of the optimum \mathbf{y} by \mathbf{d}_i multiplied by the global mutation step-size σ (line 11). The rationale behind parameterizing the sampling distribution by $\mathcal{N}(\mathbf{y}, \sigma^2 \mathbf{C})$ and not just $\mathcal{N}(\mathbf{y}, \mathbf{C})$, i.e., decoupling \mathbf{C} and σ , lies in the observation that σ can be learned more quickly and more robustly than \mathbf{C} and its adaptation alone enables linear convergence on scale-invariant problems [20].

ESs are invariant to rank-preserving / strictly monotonic transformations of f -values because all operations are based on ranks of evaluated solutions. The estimate of the optimum \mathbf{y} is updated by a weighted sum of mutation steps taken by the top ranked μ out of λ solutions (line 12). The recent analysis [2] demonstrated that the optimal recombination weights \mathbf{w} for Sphere function (see Table 1) are independent of the Hessian matrix, and hence optimal for all convex quadratic functions.

The currently most commonly applied adaptation rule for the step size is the cumulative step-size adaptation (CSA) mechanism [16]. It is based on the length of an evolution path \mathbf{p}_σ , an exponentially fading record of recent most successful steps $\mathbf{z}_{i:\lambda}$ (see line 13). If the path becomes too long (the expected path length of a Gaussian random walk can be approximated by \sqrt{n} when n is large), indicating that recent steps tend to move into the same direction, then the step size is increased. On the contrary, a too short path indicating oscillations due to overjumping the optimum results in a reduction of the step size. Rigorous analysis of CSA with and without cumulation is given in [7].

The seminal CMA-ES algorithm [15, 14] introduced adaptation of the covariance matrix, which renders the algorithm invariant to linear transformations of the search space (achieved in practice after an initial adaptation phase) and hence enables a fast convergence rate independent of the conditioning of the problem, resembling second order methods. The covariance matrix is adapted towards a weighted maximum likelihood estimate of the μ most successful samples (rank- μ update) with learning rate c_μ and a second evolution path (rank-1 update) with learning rate c_1 (see line 15); this

¹Of course, the transformation matrix needed for sampling the multivariate Gaussian is kept, enabling variable metric optimization.

update has an alternative interpretation as a stochastic gradient step on the information geometric manifold forming the algorithm’s state space [4, 29]. While the default hyperparameter values of CMA-ES given in Algorithm 1 are known to be robust, their optimal values can be adapted online during the optimization process attempting to provide an additional level of invariance [28].

Most implementations of CMA-ES consider eigendecomposition procedures of $\mathcal{O}(n^3)$ time complexity per call to obtain $\sqrt{\mathbf{C}}$ from \mathbf{C} only every n/λ iterations (see line 7) to achieve amortized $\mathcal{O}(n^2)$ time complexity per sampled solution. Numerical stability of the $\mathcal{O}(n^2)$ update can be ensured by maintaining a triangular Cholesky factor [24].

The recently proposed Matrix Adaptation Evolution Strategy (MA-ES) greatly simplifies CMA-ES by avoiding the construction of the covariance matrix \mathbf{C} . Instead it maintains only a transformation matrix \mathbf{M} representing $\sqrt{\mathbf{C}}$. After removing the approximate redundancy of \mathbf{p}_σ and \mathbf{p}_c , \mathbf{M} can be updated multiplicatively (line 16). Matrix multiplication is an $\mathcal{O}(n^3)$ operation, therefore we propose to replace the multiplicative update at iteration t by the equivalent additive update

$$\mathbf{M}^{(t+1)} \leftarrow \left(1 - \frac{c_1}{2} - \frac{c_\mu}{2}\right) \mathbf{M}^{(t)} + \frac{c_1}{2} \mathbf{d}_\sigma^{(t)} (\mathbf{p}_\sigma^{(t)})^T + \frac{c_\mu}{2} \sum_{i=1}^{\mu} w_i \mathbf{d}_{i:\lambda}^{(t)} (\mathbf{z}_{i:\lambda}^{(t)})^T, \quad (2)$$

which achieves $\mathcal{O}(n^2)$ time cost thanks to precomputing $\mathbf{d}_\sigma^{(t)} = \mathbf{M}^{(t)} \mathbf{p}_\sigma^{(t)}$ and reusing $\mathbf{d}_{i:\lambda}^{(t)}$ vectors. The resulting algorithm is referred to as *fast MA-ES*.

3 The Limited-Memory Matrix Adaptation Evolution Strategy

A number of methods was proposed to reduce the space and time complexity per sample from $\mathcal{O}(n^2)$ to $\mathcal{O}(n)$ or at least $\mathcal{O}(n \log(n))$ while still modeling the most relevant aspects of the full covariance matrix. Simple approaches like [33] restrict the covariance matrix to its diagonal, while more elaborate methods use a low-rank approach [37, 26]. Both approaches can be combined [1]. Inspired by the Limited-Memory CMA-ES [26] which in turn is inspired by the L-BFGS method [25], we show how to scale up MA-ES to high-dimensional problems. The derivation given below is based on the multiplicative update, the final result for the additive update (2) is equivalent when $\mathbf{d}_\sigma^{(t)}$ is not stored but reconstructed as $\mathbf{M}^{(t)} \mathbf{p}_\sigma^{(t)}$. At iteration t , the main update equation of MA-ES reads

$$\mathbf{M}^{(t+1)} \leftarrow \mathbf{M}^{(t)} \left[\mathbf{I} + \frac{c_1}{2} \left(\mathbf{p}_\sigma^{(t+1)} (\mathbf{p}_\sigma^{(t+1)})^T - \mathbf{I} \right) + \frac{c_\mu}{2} \left(\sum_{i=1}^{\mu} w_i \mathbf{z}_{i:\lambda}^{(t)} (\mathbf{z}_{i:\lambda}^{(t)})^T - \mathbf{I} \right) \right], \quad (3)$$

where $\mathbf{M}^{(t)}$ is adapted multiplicatively based on the rank-one update weighted by $\frac{c_1}{2}$ and the rank- μ update weighted by $\frac{c_\mu}{2}$, starting from $\mathbf{M}^{(t=0)} = \mathbf{I}$. By omitting the rank- μ update for the sake of simplicity (i.e., by setting $c_\mu = 0$), we obtain

$$\mathbf{M}^{(1)} \leftarrow \mathbf{I} + \frac{c_1}{2} \left(\mathbf{p}_\sigma^{(1)} (\mathbf{p}_\sigma^{(1)})^T - \mathbf{I} \right) = \left(1 - \frac{c_1}{2}\right) \mathbf{I} + \frac{c_1}{2} \mathbf{p}_\sigma^{(1)} (\mathbf{p}_\sigma^{(1)})^T \quad (4)$$

The sampling procedure of the i -th solution $\mathbf{x}_i^{(1)}$ follows

$$\mathbf{x}_i^{(1)} \leftarrow \mathbf{y}^{(1)} + \sigma^{(1)} \mathbf{d}_i^{(1)} = \mathbf{y}^{(1)} + \sigma^{(1)} \mathbf{M}^{(1)} \mathbf{z}_i^{(1)}, \quad (5)$$

where $\mathbf{z}_i^{(1)} \sim \mathcal{N}(\mathbf{0}, \mathbf{I})$. One can rewrite $\mathbf{d}_i^{(1)} = \mathbf{M}^{(1)} \mathbf{z}_i^{(1)}$ based on equation (4) as

$$\mathbf{d}_i^{(1)} = \mathbf{M}^{(1)} \mathbf{z}_i^{(1)} = \left(\left(1 - \frac{c_1}{2}\right) \mathbf{I} + \frac{c_1}{2} \mathbf{p}_\sigma^{(1)} (\mathbf{p}_\sigma^{(1)})^T \right) \mathbf{z}_i^{(1)} = \mathbf{z}_i^{(1)} \left(1 - \frac{c_1}{2}\right) + \frac{c_1}{2} \mathbf{p}_\sigma^{(1)} \left((\mathbf{p}_\sigma^{(1)})^T \mathbf{z}_i^{(1)} \right) \quad (6)$$

Importantly, $\left((\mathbf{p}_\sigma^{(1)})^T \mathbf{z}_i^{(1)} \right)$ is a scalar (see line 10 in Algorithm 1) and thus equation (6) does not require $\mathbf{M}^{(1)}$ to be stored in memory. One generally obtains

$$\mathbf{d}_i^{(t)} = \mathbf{M}^{(t)} \mathbf{z}_i^{(t)} = \mathbf{M}^{(t-1)} \underbrace{\mathbf{P}^{(t)} \mathbf{z}_i^{(t)}}_{:=\mathbf{P}^{(t)}} = \mathbf{M}^{(t-1)} \left(\left(1 - \frac{c_1}{2}\right) \mathbf{I} + \frac{c_1}{2} \mathbf{p}_\sigma^{(t)} (\mathbf{p}_\sigma^{(t)})^T \right) \mathbf{z}_i^{(t)} \quad (7)$$

Algorithm 1 CMA-ES, MA-ES and LM-MA-ES

- 1: **given** $n \in \mathbb{N}_+$, $\lambda = 4 + \lfloor 3 \ln n \rfloor$, $\mu = \lfloor \lambda/2 \rfloor$, $w_i = \frac{\ln(\mu + \frac{1}{2}) - \ln i}{\sum_{j=1}^{\mu} (\ln(\mu + \frac{1}{2}) - \ln j)}$ for $i = 1, \dots, \mu$, $\mu_w = \frac{1}{\sum_{i=1}^{\mu} w_i^2}$, $c_\sigma = \frac{\mu_w + 2}{n + \mu_w + 5}$, $c_c = \frac{4}{n + 4}$, $c_1 = \frac{2}{(n + 1.3)^2 + \mu_w}$, $c_\mu = \min\left(1 - c_1, \frac{2(\mu_w - 2 + 1/\mu_w)}{(n + 2)^2 + \mu_w}\right)$,
 $m = 4 + \lfloor 3 \ln n \rfloor$, $c_\sigma = \frac{2\lambda}{n}$, $c_{d,i} = \frac{1}{1.5^{i-1}n}$, $c_{c,i} = \frac{\lambda}{4^{i-1}n}$ for $i = 1, \dots, m$
 - 2: **initialize** $t \leftarrow 0$, $\mathbf{y}^{(t=0)} \in \mathbb{R}^n$, $\sigma^{(t=0)} > 0$, $\mathbf{p}_\sigma^{(t=0)} = \mathbf{0}$, $\mathbf{p}_c^{(t=0)} = \mathbf{0}$, $\mathbf{C}^{(t=0)} = \mathbf{I}$, $\mathbf{M}^{(t=0)} = \mathbf{I}$,
 $\mathbf{m}_i^{(t=0)} \in \mathbb{R}^n$, $\mathbf{m}_i^{(t=0)} = \mathbf{0}$ for $i = 1, \dots, m$
 - 3: **repeat**
 - 4: **for** $i \leftarrow 1, \dots, \lambda$ **do**
 - 5: $\mathbf{z}_i^{(t)} \leftarrow \mathcal{N}(\mathbf{0}, \mathbf{I})$
 - 6: $\mathbf{d}_i^{(t)} \leftarrow \mathbf{z}_i^{(t)}$
 - 7: **if** $t \bmod \frac{n}{\lambda} = 0$ **then** $\mathbf{M}^{(t)} \leftarrow \sqrt{\mathbf{C}^{(t)}}$ **else** $\mathbf{M}^{(t)} \leftarrow \mathbf{M}^{(t-1)}$ ▷ CMA-ES
 - 8: $\mathbf{d}_i^{(t)} \leftarrow \mathbf{M}^{(t)} \mathbf{d}_i^{(t)}$ ▷ CMA-ES and MA-ES
 - 9: **for** $j \leftarrow 1, \dots, \min(t, m)$ **do** ▷ LM-MA-ES
 - 10: $\mathbf{d}_i^{(t)} \leftarrow (1 - c_{d,j})\mathbf{d}_i^{(t)} + c_{d,j}\mathbf{m}_j^{(t)} \left((\mathbf{m}_j^{(t)})^T \mathbf{d}_i^{(t)} \right)$ ▷ LM-MA-ES
 - 11: $\mathbf{f}_i^{(t)} \leftarrow f(\mathbf{y}^{(t)} + \sigma^{(t)}\mathbf{d}_i^{(t)})$
 - 12: $\mathbf{y}^{(t+1)} \leftarrow \mathbf{y}^{(t)} + \sigma^{(t)} \sum_{i=1}^{\mu} w_i \mathbf{d}_{i:\lambda}^{(t)}$ ▷ the symbol $i : \lambda$ denotes i -th best sample on f
 - 13: $\mathbf{p}_\sigma^{(t+1)} \leftarrow (1 - c_\sigma)\mathbf{p}_\sigma^{(t)} + \sqrt{\mu_w c_\sigma (2 - c_\sigma)} \sum_{i=1}^{\mu} w_i \mathbf{z}_{i:\lambda}^{(t)}$
 - 14: $\mathbf{p}_c^{(t+1)} \leftarrow (1 - c_c)\mathbf{p}_c^{(t)} + \sqrt{\mu_w c_c (2 - c_c)} \sum_{i=1}^{\mu} w_i \mathbf{d}_{i:\lambda}^{(t)}$ ▷ CMA-ES
 - 15: $\mathbf{C}^{(t+1)} \leftarrow (1 - c_1 - c_\mu)\mathbf{C}^{(t)} + c_1 \mathbf{p}_c (\mathbf{p}_c^{(t)})^T + c_\mu \sum_{i=1}^{\mu} w_i \mathbf{d}_{i:\lambda}^{(t)} (\mathbf{d}_{i:\lambda}^{(t)})^T$ ▷ CMA-ES
 - 16: $\mathbf{M}^{(t+1)} \leftarrow \mathbf{M}^{(t)} \left[\mathbf{I} + \frac{c_1}{2} \left(\mathbf{p}_\sigma^{(t)} (\mathbf{p}_\sigma^{(t)})^T - \mathbf{I} \right) + \frac{c_\mu}{2} \left(\sum_{i=1}^{\mu} w_i \mathbf{z}_{i:\lambda}^{(t)} (\mathbf{z}_{i:\lambda}^{(t)})^T - \mathbf{I} \right) \right]$ ▷ MA-ES
 - 17: **for** $i \leftarrow 1, \dots, m$ **do** ▷ LM-MA-ES
 - 18: $\mathbf{m}_i^{(t+1)} \leftarrow (1 - c_{c,i})\mathbf{m}_i^{(t)} + \sqrt{\mu_w c_{c,i} (2 - c_{c,i})} \sum_{j=1}^{\mu} w_j \mathbf{z}_{j:\lambda}^{(t)}$ ▷ LM-MA-ES
 - 19: $\sigma^{(t+1)} \leftarrow \sigma^{(t)} \cdot \exp \left[\frac{c_\sigma}{2} \left(\frac{\|\mathbf{p}_\sigma^{(t+1)}\|^2}{n} - 1 \right) \right]$
 - 20: $t \leftarrow t + 1$
 - 21: **until** *stopping criterion is met*
-

leading to a sequence of products

$$\begin{aligned} \mathbf{d}_i^{(t)} &= \left(\left(1 - \frac{c_1}{2} \right) \mathbf{I} + \frac{c_1}{2} \mathbf{p}_\sigma^{(1)} (\mathbf{p}_\sigma^{(1)})^T \right) \cdots \\ &\cdots \left(\left(1 - \frac{c_1}{2} \right) \mathbf{I} + \frac{c_1}{2} \mathbf{p}_\sigma^{(t-1)} (\mathbf{p}_\sigma^{(t-1)})^T \right) \cdot \left(\left(1 - \frac{c_1}{2} \right) \mathbf{I} + \frac{c_1}{2} \mathbf{p}_\sigma^{(t)} (\mathbf{p}_\sigma^{(t)})^T \right) \mathbf{z}_i^{(t)} \end{aligned} \quad (8)$$

which is to be treated from right to left. Thus, the sampling procedure for $\mathbf{d}_i^{(t)} = \mathbf{M}^{(t)} \mathbf{z}_i^{(t)}$ does neither require matrix-matrix-product operations nor does it require the storage of $\mathbf{M}^{(t)} \in \mathbb{R}^{n \times n}$, but can be performed based on t vectors $\mathbf{p}_\sigma^{(t)}$ used to construct $\mathbf{M}^{(t)}$. However, this is efficient only for $t \ll n$. Therefore, in order to reduce the cost of the sampling procedure, equation (8) must be *approximated* in one way or another by artificially limiting the number m of supporting $\mathbf{p}_\sigma^{(t)}$ vectors such that $m \ll n$. In this work we pick $m \in \mathcal{O}(\log(n))$.

LM-CMA-ES[26] addresses a similar problem of compactly representing the covariance matrix with $m \in \mathcal{O}(\log(n))$ direction vectors: instead of considering the last m vectors, it samples them in a certain temporal distance in terms of iterations t . The same approach works for LM-MA-ES (see

section 1 and Algorithm 1 in the supplementary material). However, the rather complicated procedure of ensuring a temporal distance between \mathbf{p}_σ vectors can be simplified by considering different time horizons of their update. This procedure is a viable alternative since \mathbf{p}_σ itself is anyway incrementally updated with $\sum_{i=1}^\mu w_i \mathbf{z}_{i:\lambda}$. Thus, instead of a full transformation matrix $\mathbf{M} \in \mathbb{R}^{n \times n}$, LM-MA-ES maintains $m \in \mathcal{O}(\log(n))$ vectors \mathbf{m}_i (see lines 17-18 in Algorithm 1), modeling the deviation of the transformation matrix from the identity as a rank- m matrix. The learning rates $c_{c,i}$ and $c_{d,i}$ for applying and updating the vectors \mathbf{m}_i are chosen to be exponentially decaying, hence the \mathbf{m}_i are fading records of mean update steps on exponentially differing time scales. This is in contrast to CMA-ES and MA-ES, which update their matrices \mathbf{C} and \mathbf{M} only with two different learning rates for the rank-1 and rank- μ updates, and hence operate on a single time scale. LM-MA-ES learns some directions very quickly, while others are kept more stable. This can be advantageous in particular in high dimensions where learning rates are generally small due to the sub-linear sample size.

The proposed LM-MA-ES method features all invariance properties of modern ESs, namely invariance to translation and rotation, as well as invariance to strictly monotonic (rank-preserving) transformations of objective values.

4 Experimental validation

With our experimental evaluation we aim to answer the following questions:

- How does LM-MA-ES compare to MA-ES, i.e., what is the effect of modeling only a $\mathcal{O}(\log(n))$ dimensional subspace?
- How does LM-MA-ES compare to other algorithms designed for high-dimensional black-box optimization?
- Is LM-MA-ES suitable for solving problems in machine learning?

To answer these questions, we investigate the performance on standard benchmark problems of varying dimension, and we generate adversarial inputs for a random forest classifier.

Name	Function $f(x)$
Sphere	$\sum_{i=1}^n x_i^2$
Ellipsoid	$\sum_{i=1}^n 10^{\frac{i-1}{n-1}} x_i^2$
Rosenbrock	$\sum_{i=1}^{n-1} (100 \cdot (x_i^2 - x_{i+1})^2 + (x_i - 1)^2)$
Discus	$10^6 x_1^2 + \sum_{i=2}^n x_i^2$
Cigar	$x_1^2 + 10^6 \sum_{i=2}^n x_i^2$
Different Powers	$\sum_{i=1}^n x_i ^{2+4(i-1)/(n-1)}$

Table 1: Test functions used in this study.

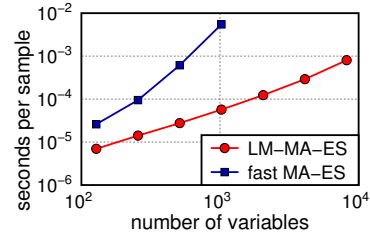


Figure 1: Internal algorithm cost.

4.1 Performance on Benchmark Problems

We experimentally validate the proposed LM-MA-ES algorithm on large-scale variants ($n \in \{128, 256, \dots, 8192\}$) of well established benchmark problems [9] (see Table 1). Starting from the initial region $[-5, 5]^n$ containing the optimum with initial step size $\sigma = 3$ we optimize until reaching the (rather exact) target precision of $f_{tar} = 10^{-10}$.

All hyperparameters of LM-MA-ES and MA-ES are given in Algorithm 1. We use LM-CMA-ES [26], VD-CMA-ES [1] and the active $(\mu/\mu_w, \lambda)$ -CMA-ES [17, 21] (aCMA-ES, known to be up to 2 times more efficient than the default CMA-ES) as baselines. The source code of LM-MA-ES is available in the supplementary material.

LM-MA-ES does not show performance degradation when applied to translated and rotated test functions (see also Figure 1 in the supplementary material). Figure 1 shows the effect of the $\mathcal{O}(n \log(n))$ scaling of the runtime per sample as compared to $\mathcal{O}(n^2)$ of fast-MA-ES (in the following denoted as MA-ES), measured for implementations of the algorithms in plain C.

The much better internal scaling is of value only if the algorithm does not pay a too high price in terms of an increased number of function evaluations required to reach f_{tar} . Therefore we test LM-MA-ES against MA-ES with full rank transformation matrix. Figure 2 shows that LM-MA-ES performs

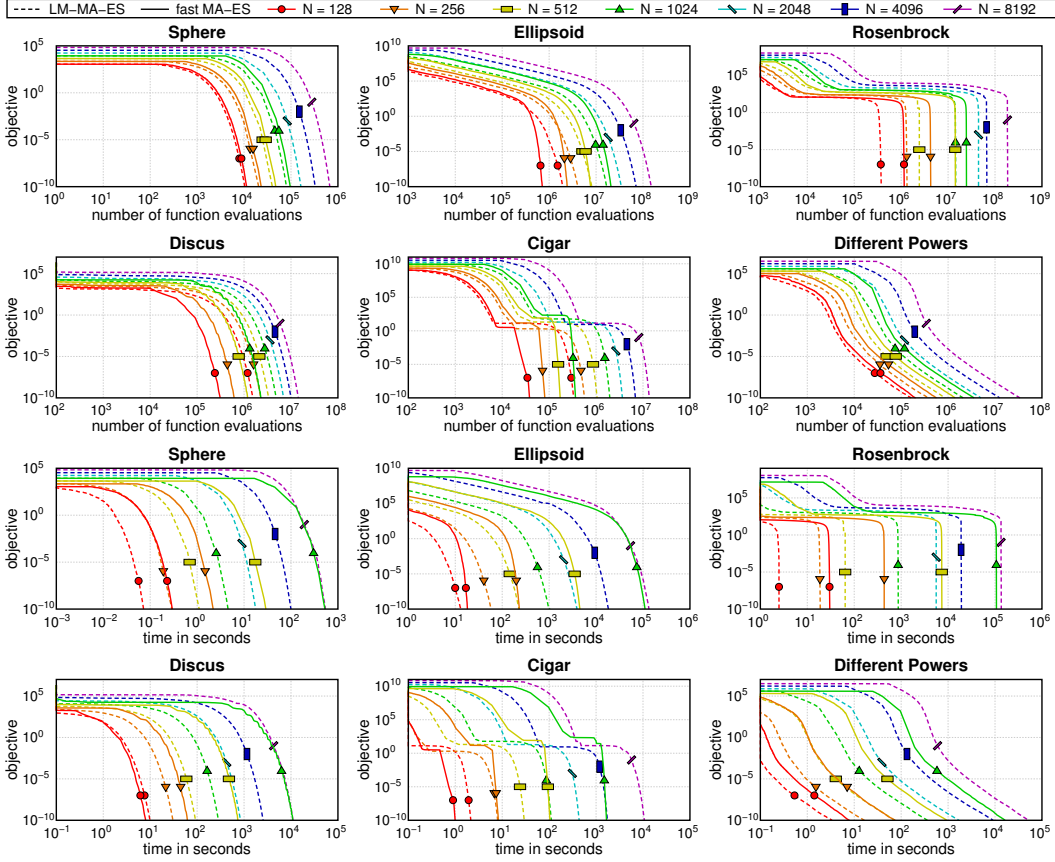


Figure 2: Runtime in number of function evaluations (rows 1–2) and seconds (rows 3–4) of LM-MA-ES in 128 to 8192 dimensions and fast MA-ES in 128 to 1024 dimensions on six standard benchmark problems.

surprisingly well: in many cases it is actually faster and this tends to happen more often for larger n . LM-MA-ES is always faster in terms of wall clock time, in some cases by a factor of 100.

Figure 3 shows that LM-MA-ES scales favorably compared to LM-CMA-ES achieving better scaling on the Rosenbrock and Discus functions, but a worse scaling on Cigar. The latter result might be due to an improper setting of the hyperparameters, a problem that can most probably be fixed with the technique proposed in [28]. VD-CMA is not able to solve some rotated functions efficiently due to the restrictions on the covariance matrix that the algorithm assumes [1, 26].

4.2 Adversarial Inputs

Several standard classifiers like the k -nearest-neighbor predictor (without distance-based weights), decision trees, and random forests are not differentiable with respect to their inputs. The predictions are piecewise constant and hence trivially piecewise differentiable, however, the gradient is zero and hence uninformative. This is a significant complication when generating adversarial inputs [38] for such classifiers, a problem for which only rather weak attacks exist [22, 40]. We compare MA-ES and LM-MA-ES on this task. To this end we train a random forest consisting of 1000 trees on the MNIST data set (784 dimensional input, 10 classes, 60,000 training points, 10,000 test points). It achieves a test error of 97.21%, which is clearly worse than the results obtained with convolutional neural networks, however, the predictor is highly non-trivial in the sense of being far from guessing performance. Let h denote the random forest predictor, let x_0 denote a correctly classified test point (of which we have 9721), and let y_0 denote the corresponding label. For an input x , the random forest predictor outputs a probability vector $h(x) \in \mathbb{R}^{10}$. We create an adversarial version of (x_0, y_0) by

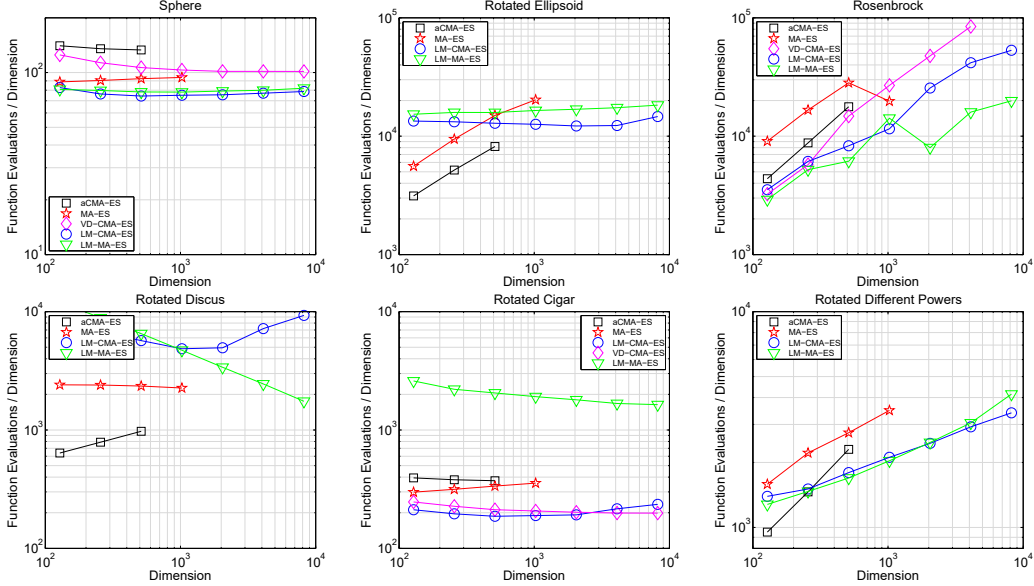


Figure 3: Median number of function evaluations (out of 5 runs) required to achieve a target objective function value of $f_{tar} = 10^{-10}$. The results of VD-CMA-ES are shown only on functions where the algorithm succeeded achieving f_{tar} . Some results for CMA-ES and MA-ES are missing due to their extremely long runtimes (note that the vertical axis shows function evaluations, not runtime).

minimizing the objective function

$$f(\mathbf{x}) = \begin{cases} h(\mathbf{x})_{y_0} - \max\{(h(\mathbf{x})_i | i \neq y_0)\} & \text{if } \mathbf{x} \text{ is classified as } y_0 \\ \frac{-1}{\|\mathbf{x} - \mathbf{x}_0\|} & \text{otherwise} \end{cases} \quad (9)$$

starting from $\mathbf{x} = \mathbf{x}_0$ with initial step size $\sigma = 1$, where an MNIST digit is encoded as a vector $\mathbf{x} \in \mathbb{R}^{784}$, with gray values in the interval $[0, 255]$. The case distinction encodes a preference for wrongly classified points: correctly classified points have a positive value, wrongly classified points have a (better) negative value. For positive values the incentive is to reduce the difference between the fraction of trees voting for the correct label y_0 and the strongest alternative. For a wrongly classified point the continuous trend moves the point back as close as possible to the original image, in terms of Euclidean distance. Note that due to invariance under rank-preserving transformations, the second term is exactly equivalent to minimization of the distance between \mathbf{x} and \mathbf{x}_0 .

Each of the 9721 optimization runs was restricted to a very low budget of 1000 objective function evaluations. This seems reasonable from a security perspective, since querying the classifier too frequently renders a remote attack inefficient. We used the sklearn implementation of the random forest [30] and implementations of MA-ES and LM-MA-ES based on numpy. The overall experiment takes about two hours for LM-MA-ES and about 7 hours for MA-ES on a laptop. The optimizers managed to turn 6152 (MA-ES) and 6321 (LM-MA-ES) images into wrongly classified inputs. In all cases, they were visually indistinguishable from the original test inputs (see Figure 4). The surprisingly high rate of about 65% of correctly classified test inputs that were successfully turned into adversarial versions demonstrates that random forests can be highly unstable and rather easy to fool by an adversarial.

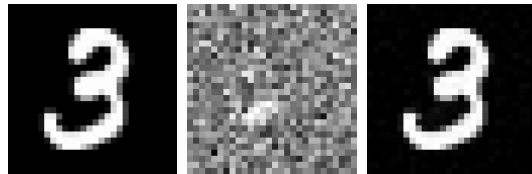


Figure 4: Original image (left) and corresponding adversarial image (right), created through a run of LM-MA-ES. The images are visually indistinguishable. The (boosted) difference image is shown in the center; mid gray corresponds to a difference of zero.

From an optimization point of view, LM-MA-ES performed clearly better than plain MA-ES. It ran about 3.5 times faster and even produced better results: in 7171 cases LM-MA-ES reached a lower objective value, while MA-ES was better in only 2550 out of 9721 cases. This is also reflected by the larger number of cases in which an adversarial input was found (6321 vs. 6152, see above).

Optimization progress over time is plotted in Figure 5 for four subsets of runs of varying difficulty. In all cases, LM-MA-ES is slightly faster. Significant differences can be observed only for the easiest problems, where MA-ES fails to improve the solution, presumably due to the small budget of objective function evaluations. In a control experiment we verified that the performance of MA-ES is only insignificantly improved compared to a simple ES without matrix adaptation, which is restricted to the adaptation of the global step size.

The better quality of the results given the same number of objective function evaluations can be explained by the low-rank structure of the LM-MA-ES steps. Adapting a full 784×784 transformation matrix with only 1000 function evaluations is a hopeless undertaking, while the top $23 = \lfloor 4 + 3 \log(784) \rfloor$ directions are much easier to adapt. This difference allows LM-MA-ES to use learning rates that are up to several orders of magnitude larger than for MA-ES, resulting in faster adaptation to the problem at hand. From the difference image in Figure 4 we clearly see a bright blob, indicating that LM-MA-ES has identified a subspace with a meaningful interpretation for the problem at hand. In contrast, the plain ES without matrix adaptation applies only white noise distortions, and this is also what’s encoded by the initial search distribution of MA-ES and LM-MA-ES.

Returning to our initial questions we conclude that LM-MA-ES successfully marries the simplicity of the update mechanisms of MA-ES with the graceful scaling of large-scale optimizers like LM-CMA-ES to large n . LM-MA-ES is competitive with MA-ES in terms of the required number of objective function evaluations, while reducing the algorithm internal cost per sample considerably from $\mathcal{O}(n^2)$ down to $\mathcal{O}(n \log(n))$. Taken together this yields in significant speed-ups for high-dimensional problems. By applying our algorithm to the problem of generating adversarial inputs for a random forest classifier, we demonstrate the value of LM-MA-ES for this domain, and uncover a surprising vulnerability of random forests with respect to the existence of adversarial inputs.

5 Conclusion

The recently proposed Matrix Adaptation Evolution Strategy is a simpler variant of the Covariance Matrix Adaptation Evolution Strategy. We showed that the $\mathcal{O}(n^2)$ time and space complexity of MA-ES, which is prohibiting for large n , can be reduced to $\mathcal{O}(n \log(n))$ adopting the approach used in [26]. The proposed Limited-Memory Matrix Adaptation Evolution Strategy matches the state-of-the-art results on large-scale optimization problems while being algorithmically simpler than LM-CMA-ES.

Future work should investigate to which extent the inclusion of the rank- μ update can improve the performance. The learning rates of LM-MA-ES can be optimized online as it is commonly done in self-adaptive evolutionary algorithms [6] or based on the maximum-likelihood principle [28].

A promising venue for LM-MA-ES would be to accelerate Stochastic Gradient Descent (SGD) for training deep neural networks by replacing the evolution path vectors by momentum vectors based on noisy batch gradients. The method could potentially represent an alternative to L-BFGS and numerous SGD variants with adaptive learning rates.

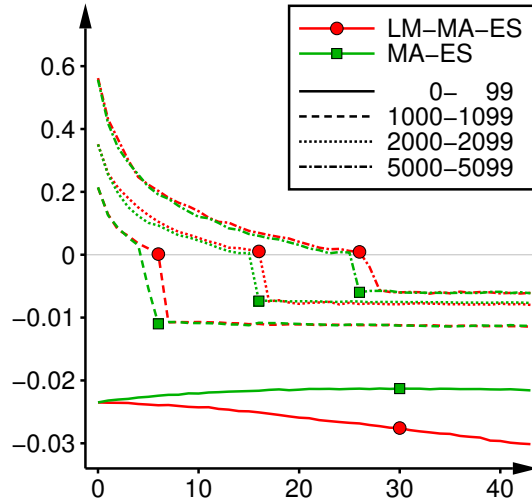


Figure 5: Progress over 1000 function evaluations (44 iterations) of LM-MA-ES and MA-ES on the task of generating adversarial inputs. The figure shows four objective function curves corresponding to equation (9) for each algorithm, referring to medians over 100 runs each. The 9721 problems were sorted by their initial objective value. We consider problems 0 to 99 (the 100 simplest problems), problems 1000 to 1099, 2000 to 2099, and 5000 to 5099.

References

- [1] Youhei Akimoto, Anne Auger, and Nikolaus Hansen. Comparison-based natural gradient optimization in high dimension. In *Genetic and Evolutionary Computation Conference*, pages 373–380. ACM, 2014.
- [2] Youhei Akimoto, Anne Auger, and Nikolaus Hansen. Quality gain analysis of the weighted recombination evolution strategy on general convex quadratic functions. In *Proceedings of the 14th ACM/SIGEVO Conference on Foundations of Genetic Algorithms*, pages 111–126. ACM, 2017.
- [3] Youhei Akimoto and Nikolaus Hansen. Online model selection for restricted covariance matrix adaptation. In *International Conference on Parallel Problem Solving from Nature*, pages 3–13. Springer, 2016.
- [4] Youhei Akimoto, Yuichi Nagata, Isao Ono, and Shigenobu Kobayashi. Bidirectional relation between cma evolution strategies and natural evolution strategies. In *International Conference on Parallel Problem Solving from Nature*, pages 154–163. Springer, 2010.
- [5] Hans-Georg Beyer. Convergence analysis of evolutionary algorithms that are based on the paradigm of information geometry. *Evolutionary Computation*, 22(4):679–709, 2014.
- [6] Hans-Georg Beyer and Kalyanmoy Deb. On self-adaptive features in real-parameter evolutionary algorithms. *IEEE Transactions on evolutionary computation*, 5(3):250–270, 2001.
- [7] Hans-Georg Beyer and Michael Hellwig. The Dynamics of Cumulative Step-Size Adaptation on the Ellipsoid Model. *Evolutionary Computation*, 24(1):25–57, 2016.
- [8] Hans-Georg Beyer and Bernhard Sendhoff. Simplify your covariance matrix adaptation evolution strategy. *IEEE Transactions on Evolutionary Computation*, 2017.
- [9] Finck Finck, Nikolaus Hansen, Raymond Ros, and Anne Auger. Real-parameter black-box optimization benchmarking 2010: Experimental setup. Technical Report 2009/21, Research Center PPE, 2010.
- [10] Tobias Glasmachers and Christian Igel. Uncertainty handling in model selection for support vector machines. In G. Rudolph, T. Jansen, S. Lucas, C. Poloni, and N. Beume, editors, *Parallel Problem Solving from Nature (PPSN)*, pages 185–194. Springer, 2008.
- [11] Faustino Gomez, Jürgen Schmidhuber, and Risto Miikkulainen. Accelerated neural evolution through cooperatively coevolved synapses. *Journal of Machine Learning Research*, 9(May):937–965, 2008.
- [12] Nikolaus Hansen, Dirk V Arnold, and Anne Auger. Evolution strategies. In *Springer Handbook of Computational Intelligence*, pages 871–898. Springer, 2015.
- [13] Nikolaus Hansen, Anne Auger, Raymond Ros, Steffen Finck, and Petr Pošík. Comparing results of 31 algorithms from the black-box optimization benchmarking BBOB-2009. In *Proceedings of the 12th annual conference companion on Genetic and evolutionary computation, GECCO 2010*, pages 1689–1696, 2010.
- [14] Nikolaus Hansen, Sibylle D. Müller, and Petros Koumoutsakos. Reducing the time complexity of the derandomized evolution strategy with covariance matrix adaptation (CMA-ES). *Evolutionary Computation*, 11(1):1–18, 2003.
- [15] Nikolaus Hansen and Andreas Ostermeier. Adapting arbitrary normal mutation distributions in evolution strategies: The covariance matrix adaptation. In *Evolutionary Computation, 1996., Proceedings of IEEE International Conference on*, pages 312–317. IEEE, 1996.
- [16] Nikolaus Hansen and Andreas Ostermeier. Completely Derandomized Self-Adaptation in Evolution Strategies. *Evolutionary Computation*, 9(2):159–195, June 2001.
- [17] Nikolaus Hansen and Raymond Ros. Benchmarking a weighted negative covariance matrix update on the BBOB-2010 noiseless testbed. In *Genetic and Evolutionary Computation Conference*, pages 1673–1680. ACM, 2010.

- [18] Verena Heidrich-Meisner and Christian Igel. Hoeffding and Bernstein races for selecting policies in evolutionary direct policy search. In *Proceedings of the 26th Annual International Conference on Machine Learning*, pages 401–408. ACM, 2009.
- [19] Christian Igel. Evolutionary kernel learning. In *Encyclopedia of Machine Learning*, pages 369–373. Springer, 2011.
- [20] Jens Jägersküpper. Rigorous runtime analysis of the $(1+1)$ ES: $1/5$ -rule and ellipsoidal fitness landscapes. In *International Workshop on Foundations of Genetic Algorithms*, pages 260–281. Springer, 2005.
- [21] Grahame A. Jastrebski and Dirk V. Arnold. Improving Evolution Strategies through Active Covariance Matrix Adaptation. In *IEEE Congress on Evolutionary Computation*, pages 2814–2821, 2006.
- [22] Alex Kantchelian, Doug Tygar, and Anthony Joseph. Evasion and hardening of tree ensemble classifiers. In *International Conference on Machine Learning*, pages 2387–2396, 2016.
- [23] James N Knight and Monte Lunacek. Reducing the space-time complexity of the CMA-ES. In *Genetic and Evolutionary Computation Conference*, pages 658–665. ACM, 2007.
- [24] Oswin Krause, Dídac Rodríguez Arbonès, and Christian Igel. CMA-ES with optimal covariance update and storage complexity. In *Advances in Neural Information Processing Systems*, pages 370–378, 2016.
- [25] Dong C Liu and Jorge Nocedal. On the limited memory BFGS method for large scale optimization. *Mathematical programming*, 45(1-3):503–528, 1989.
- [26] Ilya Loshchilov. LM-CMA: An alternative to L-BFGS for large-scale black box optimization. *Evolutionary Computation*, 25(1):143–171, 2017.
- [27] Ilya Loshchilov and Frank Hutter. CMA-ES for Hyperparameter Optimization of Deep Neural Networks. *arXiv preprint arXiv:1604.07269*, 2016.
- [28] Ilya Loshchilov, Marc Schoenauer, Michele Sebag, and Nikolaus Hansen. Maximum Likelihood-based Online Adaptation of Hyper-parameters in CMA-ES. In *Parallel Problem Solving from Nature—PPSN*, pages 70–79. Springer, 2014.
- [29] Yann Ollivier, Ludovic Arnold, Anne Auger, and Nikolaus Hansen. Information-geometric optimization algorithms: A unifying picture via invariance principles. *Journal of Machine Learning Research*, 18(18):1–65, 2017.
- [30] Fabian Pedregosa, Gaël Varoquaux, Alexandre Gramfort, Vincent Michel, Bertrand Thirion, Olivier Grisel, Mathieu Blondel, Peter Prettenhofer, Ron Weiss, Vincent Dubourg, Jake Vanderplas, Alexandre Passos, David Cournapeau, Matthieu Brucher, Matthieu Perrot, and Édouard Duchesnay. Scikit-learn: Machine learning in Python. *Journal of Machine Learning Research*, 12:2825–2830, 2011.
- [31] Leonard Rastrigin. *In the world of random events*. Latvian Academy of Science, USSR, Riga, 1963.
- [32] Ingo Rechenberg. *Evolutionsstrategie: Optimierung technischer Systeme nach Prinzipien der biologischen Evolution*. Frommann-Holzboog, 1973.
- [33] Raymond Ros and Nikolaus Hansen. A simple modification in CMA-ES achieving and space complexity. In *Parallel Problem Solving from Nature—PPSN*, pages 296–305. Springer, 2008.
- [34] Tim Salimans, Jonathan Ho, Xi. Chen, and Ilya Sutskever. Evolution strategies as a scalable alternative to reinforcement learning. Technical Report arXiv:1703.03864, arxiv.org, 2017.
- [35] David Shanno. Conditioning of Quasi-Newton Methods for Function Minimization. *Math. of Computation*, 24(111):647–656, 1970.
- [36] Freck Stulp and Olivier Sigaud. Robot skill learning: From reinforcement learning to evolution strategies. *Paladyn, Journal of Behavioral Robotics*, 4(1):49–61, 2013.

- [37] Yi Sun, Faustino Gomez, Tom Schaul, and Juergen Schmidhuber. A linear time natural evolution strategy for non-separable functions. *arXiv preprint arXiv:1106.1998*, 2011.
- [38] Christian Szegedy, Wojciech Zaremba, Ilya Sutskever, Joan Bruna, Dumitru Erhan, Ian Goodfellow, and Rob Fergus. Intriguing properties of neural networks. Technical Report arXiv:1312.6199, arxiv.org, 2013.
- [39] Daan Wierstra, Tom Schaul, Tobias Glasmachers, Yi Sun, Jan Peters, and Jürgen Schmidhuber. Natural evolution strategies. *The Journal of Machine Learning Research*, 15(1):949–980, 2014.
- [40] Weilin Xu, Yanjun Qi, and David Evans. Automatically evading classifiers. In *Proceedings of the 2016 Network and Distributed Systems Symposium*, 2016.

Supplementary Material for the paper **Limited-Memory Matrix Adaptation for Large Scale Black-box Optimization**

I LM-MA-ES with the same procedure to store direction vectors as in LM-CMA-ES

As it is mentioned in the main text of the paper, our original approach to design LM-MA-ES was to employ the same procedure to storage direction vectors as used in LM-CMA-ES [26]. The corresponding variant of LM-MA-ES with $O(m_{\max}n)$ time and space complexity is given below in Algorithm 1.

Instead of $\mathbf{M}^{(t)} \in \mathbb{R}^{n \times n}$ used in the original MA-ES, we employ a storage matrix $\mathbf{M}^{(t)} \in \mathbb{R}^{m_{\max} \times n}$ whose lines store the evolution path vectors computed at different iterations of the algorithm. While the original MA-ES employs $\mathbf{p}_\sigma^{(t)}$ to adapt both $\sigma^{(t)}$ and $\mathbf{M}^{(t)}$, we note that the optimal time horizon of the two processes can be different. Therefore, we separately adapt $\mathbf{p}_\sigma^{(t)}$ with the learning rate $c_\sigma = \frac{1}{m_{\max}}$ and $\mathbf{p}_c^{(t)}$ with the learning rate $c_c = \frac{1}{n}$ (see lines 14 and 15, respectively). At the first m_{\max} iterations of the algorithm, LM-MA works as MA-ES without the rank- μ update, i.e., with $c_\mu = 0$, and a different setting for hyperparameters, e.g., $c_c \neq c_\sigma$. The equivalence is due to the use of the first m_{\max} evolution path vectors $\mathbf{p}_c^{(t)}$ to reproduce $\mathbf{M}^{(t=m_{\max})}$ based on the the rank-one update exactly. When $m_{\max} < n$, one can greatly reduce the time and space complexity of the final algorithm. However, the use of the most recent m_{\max} evolution path vectors would lead to a degenerative sampling. Therefore, following [26], we adopt a reference array *ref* (thought of as a matrix, storing one vector per row) to access $\mathbf{p}_c^{(t)}$ vectors in $\mathbf{M}^{(t)}$ such that the i -th line of $\mathbf{M}^{(t)}$, i.e., $\mathbf{M}_{ref_i}^{(t)}$, belongs to the i -th oldest vector (in terms of its iteration index t) among the stored ones (see line 25). In order to well approximate the effect that would be obtained with the full matrix based on the rank-one update, we force the storage to support a temporal distance between the evolution path vectors such that the temporal distance $\mathit{time}_{ref_{i+1}} - \mathit{time}_{ref_i}$ between $i + 1$ -th and i -th vectors is not greater than $N_i = n^2/m_{\max}$ (see lines 20-22). This procedure replaces the vector with the smallest temporal distance to its older neighbor by the most recent vector $\mathbf{p}_c^{(t+1)}$ (see line 25). Periodically, the oldest vector is also removed to constrain the distance according to N (see line 22). The step-size adaptation of LM-MA-ES is the same as in MA-ES and CMA-ES, i.e., based on the cumulative step-size adaptation (CSA) rule of [15] (see line 26).

As it is mentioned in section 3 of the main paper, we found that instead of a rather complicated procedure described in this section, one can continuously update a set of m vectors that is distantly similar to computing momentum vectors in Stochastic Gradient Descent. The idea was born while attempting to implement Algorithm 1 for training deep neural networks. Since the performance of both algorithms is comparable, we decided to present the simpler one (given in the main paper) as our main method.

II Invariance

LM-MA-ES, just like MA-ES, is invariant to translation, rotation and scaling of the objective function in search space, provided that the initial search distribution is transformed accordingly. However, in order to justify the use of separable test functions in the experimental evaluation, we validate this property empirically, by showing median runs (out of 5 runs) of the algorithm on separable and rotated problems. Figure 1 shows convergence curves. The only systematic effect is due to initialization in the hypercube $[-5, 5]^n$, which is not rotated. The deviations are minimal, and no larger than the usual deviations due to randomized initialization and operation of the algorithm. This is in contrast to VD-CMA-ES [1], which is unable to solve rotated versions of some of the test problems.

Algorithm 1 LM-MA-ES with the same procedure to store direction vectors as in LM-CMA-ES

1: **given** $n \in \mathbb{N}_+$, $m_{max} = 4 + \lfloor 3 \ln n \rfloor$, $\lambda = 4 + \lfloor 3 \ln n \rfloor$, $\mu = \lfloor \lambda/2 \rfloor$, $w_i = \frac{\ln(\mu + \frac{1}{2}) - \ln i}{\sum_{j=1}^{\mu} (\ln(\mu + \frac{1}{2}) - \ln j)}$ for $i = 1, \dots, \mu$, $\mu_w = \frac{1}{\sum_{i=1}^{\mu} w_i^2}$, $c_1 = \frac{1}{n}$, $c_\sigma = \frac{1}{m_{max}}$, $c_c = \frac{1}{n}$, $d_\sigma = 0.5$,
 2: **initialize** $t \leftarrow 0$, $\mathbf{y}^{(t=0)} \in \mathbb{R}^n$, $m^{(t=0)} = 0$, $\sigma^{(t=0)} > 0$, $\mathbf{p}_\sigma^{(t=0)} = \mathbf{0}$, $\mathbf{p}_c^{(t=0)} = \mathbf{0}$, $\mathbf{M} \in \mathbb{R}^{m_{max} \times n}$, $\mathbf{ref} \in \mathbb{N}_+^{m_{max}}$, $\mathbf{time} \in \mathbb{N}_+^{m_{max}}$, $\mathbf{N} \in \mathbb{N}_+^{m_{max}-1} = n^2/m_{max}$
 3: **repeat**
 4: **for** $i \leftarrow 1, \dots, \lambda$ **do**
 5: $\mathbf{z}_i^{(t)} \leftarrow \mathcal{N}(\mathbf{0}, \mathbf{I})$
 6: $\mathbf{d}_i^{(t)} \leftarrow \mathbf{z}_i^{(t)}$
 7: **for** $j \leftarrow m^{(t)}, \dots, 1$ **do**
 8: $c \leftarrow c_1$
 9: **if** $j < m^{(t)}$ **then**
 10: $c_1 \leftarrow c_1(\mathbf{time}_{ref_{j+1}} - \mathbf{time}_{ref_j})/N_j$
 11: $\mathbf{d}_i^{(t)} \leftarrow (1 - c_1)\mathbf{d}_i^{(t)} + c_1\mathbf{M}_{ref_j} \left(\sum_{k=1}^n \mathbf{M}_{ref_j, k} \mathbf{d}_{i, k}^{(t)} \right)$
 12: $\mathbf{f}_i^{(t)} \leftarrow f(\mathbf{y}^{(t)} + \sigma^{(t)}\mathbf{d}_i^{(t)})$
 13: $\mathbf{y}^{(t+1)} \leftarrow \mathbf{y}^{(t)} + \sigma^{(t)} \sum_{i=1}^{\mu} w_i \mathbf{d}_{i:\lambda}^{(t)}$ // the symbol $i : \lambda$ denotes i -th best sample on f
 14: $\mathbf{p}_\sigma^{(t+1)} \leftarrow (1 - c_\sigma)\mathbf{p}_\sigma^{(t)} + \sqrt{\mu_w c_\sigma (2 - c_\sigma)} \sum_{i=1}^{\mu} w_i \mathbf{z}_{i:\lambda}^{(t)}$
 15: $\mathbf{p}_c^{(t+1)} \leftarrow (1 - c_c)\mathbf{p}_c^{(t)} + \sqrt{\mu_w c_c (2 - c_c)} \sum_{i=1}^{\mu} w_i \mathbf{z}_{i:\lambda}^{(t)}$
 16: $m^{(t+1)} \leftarrow \min(t + 1, m_{max})$
 17: **if** $(t < m_{max})$ **then**
 18: $ref_{m^{(t+1)}} \leftarrow t + 1$
 19: **else**
 20: $i_{min} \leftarrow \operatorname{argmin}_i \left(\mathbf{time}_{ref_{i+1}} - \mathbf{time}_{ref_i} - N_i \right)$, $|1 \leq i \leq (m^{(t+1)} - 1)$
 21: **if** $\left(\mathbf{time}_{ref_{i_{min}+1}} - \mathbf{time}_{ref_{i_{min}}} - N_{i_{min}} \geq 0 \right)$ **then**
 22: $i_{min} \leftarrow 0$
 23: remove $(i_{min} + 1)$ -th element of \mathbf{ref} and insert it at now empty m^{t+1} -th position
 24: $\mathbf{time}_{ref_{m^{(t+1)}}} \leftarrow t + 1$
 25: $\mathbf{M}_{ref_{m^{(t+1)}}} \leftarrow \mathbf{p}_c^{(t+1)}$
 26: $\sigma^{(t+1)} \leftarrow \sigma^{(t)} \exp \left[\frac{c_\sigma}{d_\sigma} \left(\frac{\|\mathbf{p}_\sigma^{(t+1)}\|^2}{n} - 1 \right) \right]$
 27: $t \leftarrow t + 1$
 28: **until** *stopping criterion is met*

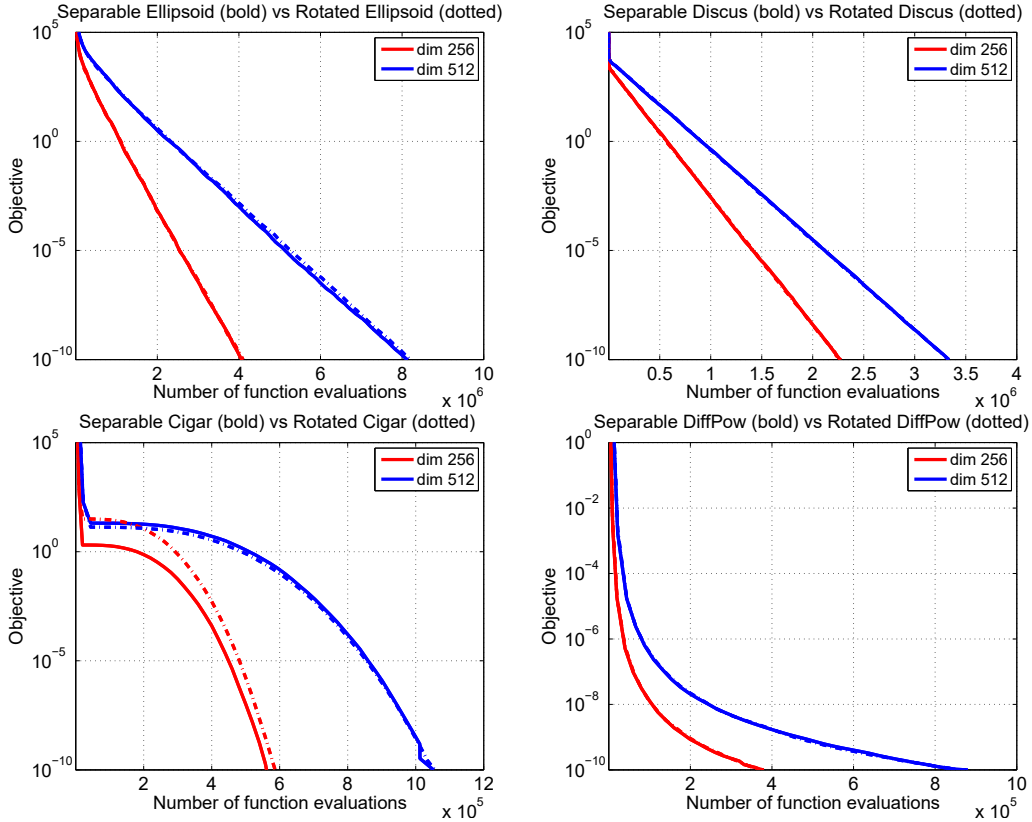


Figure 1: The trajectories show the median of 5 runs of LM-MA-ES on separable (bold lines) and rotated (dotted lines) versions of Ellipsoid, Discus, Cigar and Different Powers functions (see Table 1 of the main paper) for problem dimensions 256 and 512. The rotated functions $f(\mathbf{R}\mathbf{x})$ are obtained from the original separable functions $f(\mathbf{x})$ by applying \mathbf{R} , an orthogonal $n \times n$ matrix with each column vector \mathbf{q}_i being a uniformly distributed unit vector implementing an angle-preserving transformation. LM-MA-ES numerically demonstrates invariance to rotations. The observed difference is due to the fact that the rotations effectively change the initial range of the search domain.